Terahertz near-field imaging of metallic subwavelength holes and hole arrays

Andreas Bitzer[a] and Markus Walther[b]
Molecular and Optical Physics, Institute of Physics, Albert-Ludwigs-Universität Freiburg, Hermann-Herder-Str. 3, D-79104 Freiburg, Germany

(Received 5 March 2008; accepted 5 May 2008; published online 9 June 2008)

Metallic microstructures are investigated by time-resolved terahertz near-field imaging. By our approach, we can directly follow field diffraction from subwavelength structures as well as coupling to the surface. Near-field images of the spectral amplitude and phase of the electric field show the formation, propagation, and attenuation of surface waves and allow us to distinguish between propagating and stationary modes. Our results show that the field enhancement in an individual hole, together with the formation of standing waves on the metal surface between the holes, are key mechanisms for the extraordinary transmission phenomenon through periodic hole arrays. © *2008 American Institute of Physics*. [DOI: 10.1063/1.2936303]

Transmission of light through perforated metallic films with subwavelength structures has raised considerable interest over the past years.[1] Especially, unexpected behaviors such as strongly enhanced transmission and wavelength filtering have been observed and extensively studied at various wavelengths extending from the visible[2] to the millimeter and submillimeter wavelength region.[3] Gaining a comprehensive understanding of the underlying mechanisms requires to monitor the near field in the vicinity of the structured surface. In contrast to studies at visible frequencies where near-field investigations with subwavelength resolution are highly challenging, experiments in the long-wavelength regime can potentially overcome such limitations.[4,5]

We report a time-resolved terahertz imaging technique which allows to measure the electric field distribution in the near field of metallic samples. At the example of terahertz pulse transmission through zero-, one-, and two-dimensional arrays of subwavelength holes, as shown in Fig. 1(a), we demonstrate the propagation, attenuation, and interference of waves in the vicinity of the sample surface.

The terahertz near-field imaging setup is based on the emission and detection of single cycle terahertz pulses by photoconductive antennas optically gated by the output of a mode-locked Ti:sapphire laser system.[6] Two off-axis parabolic mirrors collimate and focus the emitted terahertz pulses onto the front side of the sample. As illustrated in Fig. 1(b), the terahertz pulses propagate through the sample and the transmitted electric field is detected. The silicon-on-sapphire detector chip is mounted with the silicon layer and the H-shaped electrodes facing the backside of the sample. The probe laser beam is focused through the sapphire substrate into the 10 μm wide photoconductive gap. The incident terahertz pulses are x polarized and the detector is oriented to be sensitive to the x component of the electric field. Spatially resolved measurements are performed by moving the detector chip together with the probe laser in x, y and z directions relative to the stationary sample and terahertz beam. The spatial resolution is limited by the finite dimensions of the probe beam focus and of the photoconductive gap between the detector electrodes and was determined to be on the order of 20 μm. Our samples consist of 300 μm thick copper plates. The minimal distance between detector and sample was experimentally limited to $z=35$ μm, which corresponds to $\sim\lambda/10$ at terahertz frequencies. In this case, the detector electrodes are close to the metal surface of the sample and capacitive coupling between detector and sample has to be considered. However, since the detector is moving over the entire image area during one measurement, any capacitive influence which is localized to the area of the photoconducitve gap becomes isotropically distributed over the image and, therefore, does not influence the characteristic of the observed field patterns.

In Fig. 2(a), we show snapshots of the electric field of a terahertz pulse transmitted through a single hole measured in a plane close to the back surface of the sample $E_x(x,y,z=35\ \mu\text{m},t)$ (upper panel) and along a cross section normal to the sample surface through the center of the hole along the x axis $E_x(x,y=0,z,t)$ (lower panel).[7] We observe the formation of a spherical wave that radiates from the hole into free space. At early times, we find that E_x is confined to the hole area, whereas two wave contributions propagate along the surface away from the hole at later times. The latter is unexpected since the boundary conditions near a perfectly conducting surface require that the surface tangential electric field $E_\parallel$ which is measured by our x polarized detector becomes zero,[8] so we would expect E_x to vanish on the metal. Since we are measuring at a slight distance from the surface, a nonvanishing tangential field could also originate from the residual tangential component of the spherical wave. In this case, however, one would expect also a nonvanishing tan-

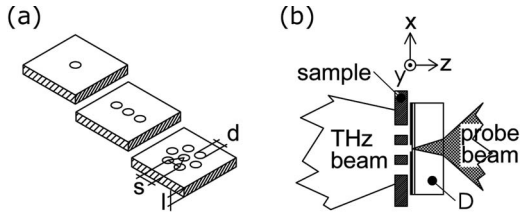

FIG. 1. (a) Investigated metal samples with $d=300$ μm, $s=450$ μm, and thickness $l=300$ μm. (b) Terahertz near-field imaging setup. The detector chip D can be translated together with the probe laser beam in x, y, and z directions relative to the stationary sample.

[a]Electronic mail: andreas.bitzer@gmail.com.
[b]Electronic mail: markus.walther@physik.uni-freiburg.de.

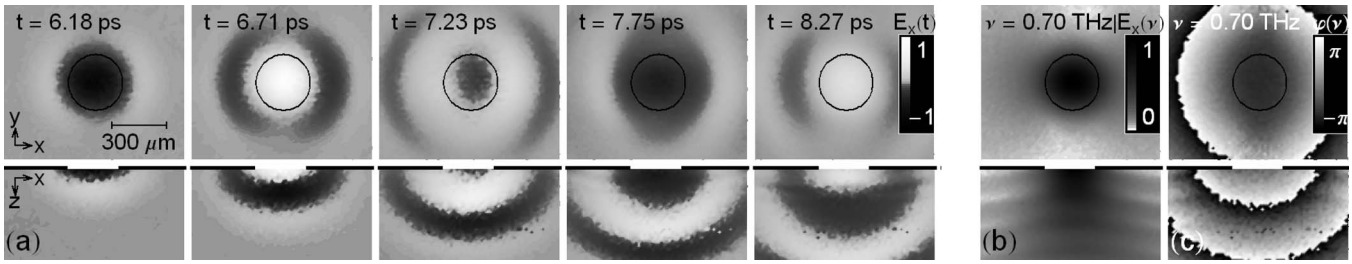

FIG. 2. (a) Time sequence of the field distribution on the backside of a subwavelength hole after illumination by a broadband terahertz pulse. Corresponding amplitude (b) and phase image (c) at a frequency of 0.7 THz.

gential field component along the y axis. In contrast, we observe strongly anisotropic field propagation mainly along the x direction. In the following, we will refer to the wave propagating along the metal as surface wave (sw) which is characterized by a considerable longitudinal field component, similar to surface plasmons in the near infrared and visible region.[9] In an additional measurement, we also examined the y component of the electric field E_y by rotating the detector by 90°. In this case, however, the signals were negligible compared to the x polarized measurements, in agreement with observations in the microwave regime.[6]

Fourier transformation of the time-dependent field distribution yields spectrally resolved amplitude and phase plots, as shown in Figs. 2(b) and 2(c) for a frequency of 0.7 THz where the amplitude spectrum of the transmitted radiation has its maximum [see Fig. 3(b)]. The amplitude distribution along the surface is strongly anisotropic according to the surface wave propagation.

Figure 2(c) shows a plot of the wrapped phase $\varphi(x,y)$, i.e., with its magnitude confined to the interval $[-\pi,\pi]$, for $\nu=0.7$ THz. Wave propagation is represented by a steadily rising phase associated with periodic jumps by 2π as a result of the phase wrapping. Since the wave vector is the gradient of the phase $\vec{k}=\nabla\varphi$, the phase jumps in the plot separated by λ represent the wave fronts of the propagating waves with $\vec{k}$ pointing orthogonally. The phase plots, therefore, indicate spherical propagation away from the hole center.

Figure 3(a) shows a spectrally and spatially resolved cross section of the incident terahertz beam profile in the focus.[10] Due to the strong frequency dependence of the beam waist, a homogeneous illumination of our samples is only given for frequencies below 1 THz. The cross section of the beam profile after transmission through the hole in Fig. 3(b), shows the low frequency cutoff of the hole below 0.59 THz. Both frequency limits define, therefore, the spectral window in which we can analyze the transmission behavior of our samples.

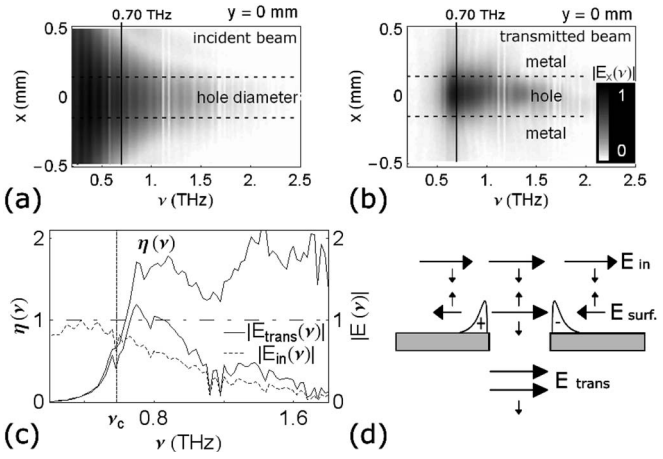

FIG. 3. [(a),(b)] Cross sections of the beam profiles $|E_x(\nu)|$ of the incident terahertz beam and after transmission through a single hole sample. The 300 μm hole diameter is indicated by the dashed lines in both plots. (c) Comparison between incident and transmitted spectral amplitude measured in the hole center. (d) Illustration of the proposed mechanism leading to enhanced transmission through a single hole in a metal plate.

In order to quantify the field transmission through the hole, we determined the amplitude spectra by a single spot measurement at the position of the center of the hole exit ($x=y=0, z=35$ μm), with the sample, $E_{\text{trans}}(\nu)$, and without, $E_{\text{in}}(\nu)$. Figure 3(c) shows both spectra together with the transmission efficiency $\eta(\nu)=E_{\text{trans}}(\nu)/E_{\text{in}}(\nu)$. Above the waveguide cutoff frequency of the hole for the dominant TE_{11}-mode at $\nu_c=1.84c/\pi d=0.59$ THz (c speed of light),[3] we observe a significantly enhanced field amplitude indicated by $\eta>1$. Note that an enhanced field transmission through single holes has been previously described[11] and is a basic aspect in the mechanism leading to extraordinary transmission through hole arrays. The transmission mechanism through the hole can be understood in terms of the excitation of surface charge oscillations and the associated formation of dipoles,[12] as sketched in Fig. 3(d). Within such a model, the incident electric field E_{in} polarizes the surface by moving surface charges on the illuminated front side of the metal. Their movement is impeded at the hole edges leading to a strong accumulation of charges which then forms an oscillating dipole over the hole area. The incident wave constructively interferes with the radiation emitted from the dipole leading to enhanced field transmission through the hole. In the backward direction, however, the field radiated from the dipole destructively contributes to the field reflected from the neighboring metal, thereby reducing the overall back reflection so that energy conservation is fulfilled.

In a second step, we investigate the interaction with radiation patterns emerging from neighboring holes. Figure 4(a) shows snapshots of the transmitted field pattern of three horizontally arranged holes, separated by $s=450$ μm, which have been coherently excited. Note that the small terahertz beam waist leads to a larger intensity entering the central hole. The amplitude spectrum shown in Fig. 4(b), exhibits stationary extrema both along the surface and in space as a result of constructive and destructive wave interference of the radiation patterns of the individual holes. In the phase plot in Fig. 4(c), the wave interference is expressed by an oscillating phase between the holes which corresponds to an alternating direction of the wave vector $\vec{k}_{\text{sw}}$ indicating counterpropagating surface waves that form a standing wave.

We finally extend our study to a two-dimensional subwavelength hole array consisting of seven hexagonally ar-

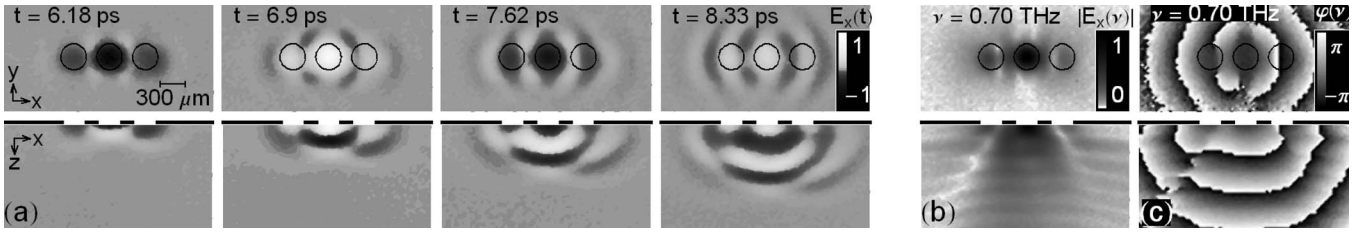

FIG. 4. (a) Time sequence of the electric field distribution measured in the near field of three linearly arranged subwavelength holes with corresponding amplitude (b) and phase images (c) at a frequency of 0.7 THz.

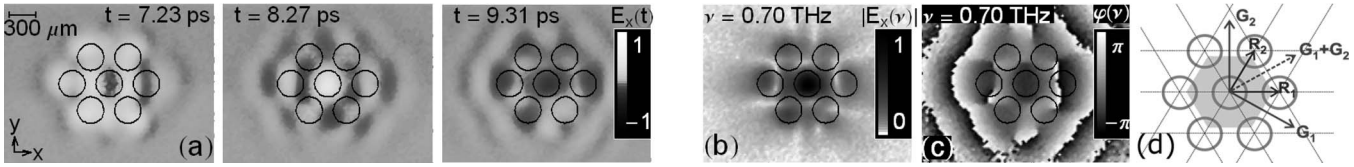

FIG. 5. Time sequence of the field transmitted through a hexagonal hole array. (b) and (c) show corresponding amplitude and phase images at ν=0.7 THz. (d) Primitive vectors of the real ($\vec{R}_1$ and $\vec{R}_2$) and the reciprocal lattice ($\vec{G}_1$ and $\vec{G}_2$). The gray area corresponds to the first Brillouin zone.

ranged holes. Figure 5(a) shows a time sequence of the x-polarized electric field close to the surface after excitation by a terahertz pulse. Under normal incidence resonant coupling of an electromagnetic wave to a surface mode in a two-dimensional grating structure occurs when the wave vector of the surface wave matches the in-plane momentum provided by the hole array $\vec{G}=i\vec{G}_1+j\vec{G}_2$, where $\vec{G}_1$ and $\vec{G}_2$ are the primitive reciprocal lattice vectors and i and j are integers.[13] This condition restricts the continuous spectrum of surface waves that emerge from a single hole to a discrete spectrum represented by wave vectors $\vec{k}_{sw}=\vec{G}$. With the primitive lattice vectors of a hexagonal lattice, as defined in Fig. 5(d), one obtains

$$|\vec{k}_{sw}| = \frac{2\pi}{s}\sqrt{\frac{4}{3}(i^2 - ij + j^2)}, \tag{1}$$

where s is the separation between the holes. At terahertz frequencies the surface wave behaves almost light like and thus, $|\vec{k}_{sw}| \approx 2\pi\nu/c \cdot \sqrt{\epsilon_d}$, with ν being the optical frequency and ϵ_d the dielectric constant of the medium in contact with the metal, in our case, air.[9] Using this approximation together with Eq. (1), one can determine the resonance frequencies of the six fundamental lattice modes at $\nu_{[\pm1,0]}=\nu_{[0,\pm1]}=\nu_{[\pm1,\pm1]}=0.77$ THz. In fact, in our measurement we observe considerably enhanced surface mode amplitudes in a spectral window around this frequency. Apart from decaying amplitudes with increasing distance from the center, the amplitude plot in Fig. 5(b) also shows pronounced stationary minima between the holes. The wrapped phase plot in Fig. 5(c) shows a wavefront pattern in the outer region of the structure which corresponds to the geometry of the lattice. Interestingly, whereas the $[\pm1,0]$ and $[\pm1,\pm1]$ fundamental modes are observed in our experiment, the waves propagating in $[0,\pm1]$ directions, i.e., normal to the incident field polarization, are absent. This unexpected behavior can be understood if we review the anisotropic surface wave pattern around a single hole with vanishing amplitudes parallel to the y axis. The discrete surface wave spectrum in a two-dimensional hole array is, therefore, the interaction of the continuous but anisotropic spectrum of surface waves emerging from a single hole with the discrete spectrum of lattice momenta. Between the holes, the phase also oscillates as an indication for standing surface waves. Therefore, the lattice represents a surface wave resonator with a discrete spectrum of eigenmodes.

In conclusion, we report a terahertz near-field imaging approach which provides time and spatially resolved measurements of the electric field distribution in the vicinity of structured samples with subwavelength spatial resolution. We use our technique to investigate terahertz pulse transmission through metallic structures consisting of subwavelength holes and hole arrays. We demonstrate enhanced transmission through a single hole as a consequence of coupling to oscillating surface charges and observe the resonant formation of stationary surface modes between a periodic arrangement of holes. Our approach for the investigation of time-dependent electric near-fields opens the way for the investigation of other interesting structures such as waveguides or resonators.

The authors acknowledge help from Hanspeter Helm, Andreas Kern and Carsten Winnewisser.

[1] C. Genet and T. W. Ebbesen, Nature (London) **445**, 39 (2007).
[2] T. W. Ebbesen, H. J. Lezec, H. F. Ghaemi, T. Thio, and P. A. Wolff, Nature (London) **391**, 667 (1998).
[3] C. Winnewisser, F. Lewen, J. Weinzierl, and H. Helm, Appl. Opt. **38**, 3961 (1999).
[4] M. A. Seo, A. J. L. Adam, J. H. Kang, J. W. Lee, S. C. Jeoung, Q. H. Park, P. C. M. Planken, and D. S. Kim, Opt. Express **15**, 11781 (2007).
[5] B. Hou, Z. H. Hang, W. J. Wen, C. T. Chan, and P. Sheng, Appl. Phys. Lett. **89**, 131917 (2006).
[6] D. Grischkowsky, S. Keiding, M. van Exter, and Ch. Fattinger, J. Opt. Soc. Am. B **7**, 2006 (1990).
[7] Movies at http://frhethz.physik.uni-freiburg.de.
[8] J. D. Jackson, *Classical Electrodynamics*, 3rd ed. (de Gruyter, Berlin, 2002).
[9] H. Raether, *Surface Plasmons on Smooth and Rough Surfaces and on Gratings* (Springer, Berlin, 1988).
[10] A. Bitzer, M. Walther, A. Kern, S. Gorenflo, and H. Helm, Appl. Phys. Lett. **90**, 071112 (2007).
[11] F. J. Garcia-Vidal, E. Moreno, J. A. Porto, and L. Martin-Moreno, Phys. Rev. Lett. **95**, 103901 (2005).
[12] X. R. Huang, R. W. Peng, Z. Wang, F. Gao, and S. S. Jiang, Phys. Rev. A **76**, 035802 (2007).
[13] T. Thio, H. F. Ghaemi, H. J. Lezec, P. A. Wolff, and T. W. Ebbesen, J. Opt. Soc. Am. B **16**, 1743 (1999).